PERGAMON

International Journal of Solids and Structures 38 (2001) 5527–5543

INTERNATIONAL JOURNAL OF SOLIDS and STRUCTURES

www.elsevier.com/locate/ijsolstr

Rapid indentation of a pre-stressed hyper-elastic half-space: comparison of axially symmetric and plane strain cases

L.M. Brock *

Department of Mechanical Engineering, University of Kentucky, 521 CRMS Building, Lexington Campus, Lexington, KY 40506-0108, USA

Received 21 June 2000; in revised form 4 October 2000

Abstract

Transient indentation of a pre-stressed hyper-elastic half-space by either a rigid smooth cone or by a rigid smooth wedge of infinite length is considered. The former represents the basis for an axially symmetric problem, the latter, for one of plane strain. The half-space is modeled as an isotropic compressible neo-Hookean material, and both cases are treated as the superposition of infinitesimal deformations upon (possibly) finite deformations due to pre-stress.

The equations for the superposed deformations exhibit the usual anisotropy induced by pre-stress, but exact expressions for the full infinitesimal fields, as well as for the dilatational, rotational and Rayleigh wave speeds in the deformed configuration, are obtained.

These demonstrate some effects of pre-stress: in particular, critical tensile pre-stress levels exist beyond which negative Poisson effects arise. Critical compressive pre-stresses also exist beyond which Rayleigh waves disappear and contact zone expansion at constant sub-critical rates cannot occur. However, the critical compressive pre-stress level is lower for the plane strain case and, indeed, this case is found to be in many respects more sensitive than the axially symmetric case to pre-stress.

Keywords: Dynamic indentation; Hyper-elastic solids; Wave speeds in deformed configuration; Pre-stress

1. Introduction

Insight into the indentation of pre-stressed hyper-elastic solids has been obtained by treating the process as the superposition of infinitesimal deformations upon the (possibly) finite deformations due to pre-stress (Green and Zerna, 1968). Beatty and Usmani (1975), in particular, used such an approach for rigid smooth punches and materials of the Hadamard type. Both analyses were static, and specific results given for axially symmetric cases. In both instances, the equations governing the infinitesimal deformations satisfied equations similar in form to those for a non-isotropic body, although the hyper-elastic solid was isotropic in the rest configuration. More recently, Brock (1999b, 2001) used the superposition approach to treat sliding

* Tel.: +1-859-257-2839; fax: +1-859-257-8057.
E-mail address: brock@engr.uky.edu (L.M. Brock).

0020-7683/01/$ - see front matter
PII: S0020-7683(00)00380-2

indentation by rigid punches on an isotropic compressible neo-Hookean material. In these instances, the analyses were steady-state dynamic, and plane-strain situations were considered.

The present study extends aspects of all these analyses in order to examine how the types of pre-stress affects solution behavior under dynamic conditions. Examples of both the transient problem of pure indentation by a rigid smooth axially symmetric cone and the corresponding plane-strain problem of a wedge of infinite length are considered. The material treated by Brock (1999b, 2001) is again chosen to represent hyper-elastic behavior, and the contact zones expand at constant sub-critical rates. Constant expansion rates give rise to homogeneity in the independent variables for the superposed infinitesimal deformations, a feature that is regularly exploited in linear elastic indentation studies (Willis, 1973; Brock, 1978).

The present study begins in Section 2 with basic equations for the superposition scheme, adopted from formulations by Beatty and Usmani (1975). The particular isotropic compressible neo-Hookean material is defined, and the plain strain and axially symmetric cases are addressed and exact transient solutions for the full field obtained, in sequence.

Both solutions show that compressive pre-stress beyond a critical value precludes the existence of Rayleigh waves and also, therefore, indentation for contact zones with sub-critical expansion rates. Moreover, all wave speeds (rotational, dilatational, Rayleigh) and the average contact zone stress in both cases are clearly influenced by pre-stress, and the effects differ in tension and compression. However, the effective elastic constants in the governing equations for the superposed infinitesimal deformations in the two cases are different, so that the pre-stress effects are different – sometimes in basic ways. Such differences also mean that the axially symmetric case does not follow directly from the plain-strain case by standard (Barber, 1996) superposition operations.

2. Basic equations

Consider an elastic body $\mathfrak{R}$ that is homogeneous and isotropic relative to an undisturbed reference configuration κ_0. A smooth motion $\mathbf{x} = \mathbf{x}(\mathbf{X})$ then takes $\mathfrak{R}$ to a deformed equilibrium configuration κ. The Cauchy stress $\mathbf{T}$ in κ is

$$\mathbf{T} = \alpha_0\mathbf{1} + \alpha_1\mathbf{B} + \alpha_2\mathbf{B}^2, \qquad \mathbf{B} = \mathbf{F}\mathbf{F}^{\mathrm{T}}, \qquad \mathbf{F} = \frac{\partial \mathbf{x}}{\partial \mathbf{X}} \tag{2.1}$$

where $(\alpha_0, \alpha_1, \alpha_2)$ are scalar-valued response functions of the principal invariants $(\mathrm{I}, \mathrm{II}, \mathrm{III})$ of $\mathbf{B}$, and body forces are absent. As noted by Beatty and Usmani (1975), experimentally based inequalities (Truesdell and Noll, 1965) tend to support the restrictions

$$\alpha_0 - \mathrm{II}\alpha_2 \leqslant 0, \quad \alpha_1 + \mathrm{I}\alpha_2 > 0, \quad \alpha_2 \leqslant 0 \tag{2.2}$$

An adjacent non-equilibrium configuration κ^* is obtained by superposing an additional, but infinitesimal, displacement $\mathbf{u}$, which depends on $\mathbf{x}$ and time. This requires an additional (incremental) Cauchy stress $\mathbf{T}' = \mathbf{T}^* - \mathbf{T}$, where $\mathbf{T}^*$ is the Cauchy stress in κ^*. To the first order in the displacement gradient $\mathbf{H} = \partial\mathbf{u}/\partial\mathbf{x}$, the components of $\mathbf{T}'$ in the principal reference system, i.e. $\mathbf{F}$ gives $\mathbf{B} = \mathrm{diag}\{\lambda_1^2, \lambda_2^2, \lambda_3^2\}$ where λ_k are the principal stretches and

$$\mathrm{I} = \lambda_1^2 + \lambda_2^2 + \lambda_3^2, \qquad \mathrm{II} = \lambda_1^2\lambda_2^2 + \lambda_3^2\lambda_1^2 + \lambda_2^2\lambda_3^2, \qquad \mathrm{III} = \lambda_1^2\lambda_2^2\lambda_3^2, \tag{2.3}$$

can be written as

$$\begin{bmatrix} T'_{11} \\ T'_{22} \\ T'_{33} \end{bmatrix} = \begin{bmatrix} \lambda'_{11} + 2\mu'_{11} & \lambda'_{12} & \lambda'_{13} \\ \lambda'_{21} & \lambda'_{22} + 2\mu'_{22} & \lambda'_{23} \\ \lambda'_{31} & \lambda'_{32} & \lambda'_{33} + 2\mu'_{33} \end{bmatrix} \begin{bmatrix} H_{11} \\ H_{22} \\ H_{33} \end{bmatrix} \tag{2.4a}$$

$$T'_{12} = \mu'_{21}H_{21} + \mu'_{12}H_{12}, \qquad T'_{23} = \mu'_{32}H_{32} + \mu'_{23}H_{23}, \qquad T'_{31} = \mu'_{13}H_{13} + \mu'_{31}H_{31} \tag{2.4b}$$

In Eqs. (2.4a) and (2.4b) the $(\lambda'_{ik}, \mu'_{ik})$ are generalized Lame′ constants defined by

$$\Gamma'_{i1} = \Gamma_{i1}\lambda_1^2, \qquad \Gamma'_{i2} = \Gamma_{i2}\lambda_2^2, \qquad \Gamma'_{i3} = \Gamma_{i3}\lambda_3^2 \tag{2.5}$$

where $i = (1, 2, 3)$, the symbol Γ represents either λ or μ, and

$$\frac{1}{2}\lambda_{ik} = \frac{\partial\alpha_0}{\partial\lambda_k^2} + \lambda_i^2\frac{\partial\alpha_1}{\partial\lambda_k^2} + \lambda_i^4\frac{\partial\alpha_2}{\partial\lambda_k^2}, \qquad \mu_{ik} = \mu_{ki} = \alpha_1 + \alpha_2\left(\lambda_i^2 + \lambda_k^2\right) \tag{2.6}$$

In κ incremental traction boundary conditions on a surface with outwardly directed normal $\mathbf{n}$ can be written in terms of the traction vector

$$\mathbf{t}^{(n)} = \mathbf{T}'\mathbf{n} + \mathbf{T}\mathbf{n}(\mathbf{n}.\mathbf{H}\mathbf{n}) - \mathbf{T}\mathbf{H}^{\mathrm{T}}\mathbf{n} \tag{2.7}$$

Finally, because κ_0 is a homogeneous configuration, the incremental balance of linear momentum reduces to (Green and Zerna, 1968)

$$\mathrm{div}\,\mathbf{T}' = \rho\ddot{\mathbf{u}} \tag{2.8}$$

where ρ is the mass density and the dot overhead denotes the (absolute) time derivative.

Consider a Hadamard material, which is characterized by the response functions

$$\alpha_0 = 2\sqrt{\mathrm{III}}\,\frac{\mathrm{d}G(\mathrm{III})}{\mathrm{dIII}}, \qquad \alpha_1 = \frac{1}{\sqrt{\mathrm{III}}}(a_0 - \mathrm{I}b_0), \qquad \alpha_2 = \frac{b_0}{\sqrt{\mathrm{III}}} \tag{2.9}$$

where (a_0, b_0) are material constants such that $b_0 = a_0 - \mu$, μ is the usual (Hibbeler, 2000) shear modulus and $G(1) = 0$. Setting $b_0 = 0$ produces the sub-class of neo-Hookean materials. In this article, the compressible case is treated; incompressibility would require that $\mathrm{III} = 1$ for all deformations. A particularly simple isotropic compressible neo-Hookean material arises when

$$G = G_0\left(\frac{1}{\sqrt{\mathrm{III}}} - 1\right) \tag{2.10}$$

where G_0 is a constant. Then Eq. (2.9) produces

$$\alpha_0 = -\frac{G_0}{\mathrm{III}}, \qquad \alpha_1 = \frac{\mu}{\sqrt{\mathrm{III}}}, \qquad \alpha_2 = 0 \tag{2.11}$$

To obtain G_0, consider $\mathfrak{R}$ to be a bar of uniform circular cross-sectional area A_0 in κ_0 that is placed in a deformed equilibrium state κ under the uniaxial load P. If the bar axis is aligned with the X_1-direction, then the Cauchy stresses for $\mathfrak{R}$ are

$$T_{11} = \frac{P}{A}, \qquad T_{22} = T_{33} = 0, \qquad T_{ik} = 0 \quad (i \neq k) \tag{2.12}$$

where A is the cross-sectional area in κ, and uniform stress is assumed. Clearly the $\mathbf{X}$ are principal axes with stretches λ_1 and $\lambda_2 = \lambda_3 = \lambda_T$, and Eqs. (2.1), (2.3) and (2.11) combine to give the formulas

$$\frac{P}{\mu A} = \sqrt{\frac{\mu}{G_0}}\lambda_1^{3/2} - \frac{1}{\lambda_1}, \qquad \lambda_T = \left(\frac{G_0}{\mu\lambda_1}\right)^{1/4} \tag{2.13}$$

Because $A = \lambda_T^2 A_0$ for homogeneous deformation, and $\lambda_1 = 1 + e_1$, where e_1 is the axial unit extension of the bar, Eq. (2.13) gives

$$\frac{P}{A_0} = \mu\left[1 + e_1 - \sqrt{\frac{G_0}{\mu}}\frac{1}{(1+e_1)^{3/2}}\right] \tag{2.14}$$

Eq. (2.14) relates a first Piola–Kirchoff stress to unit extension, and the right-hand side will appropriately vanish for $e_1 = 0$ when

$$G_0 = \mu \tag{2.15}$$

Thus, Eq. (2.11) defines a one-parameter solid, and the restriction set (2.2) is indeed satisfied. A schematic of Eq. (2.14) in view of Eq. (2.15) is given in Fig. 1, i.e. Fig. 1 represents the stress–strain curve for the material. The effective Young's modulus E^e and Poisson's ratio v^e then follow from Eqs. (2.5)–(2.7) and the slope of Eq. (2.14) as

$$\frac{E^e}{\mu} = 1 + \frac{3}{2(1+e_1)^{5/2}}, \qquad v^e = -\frac{\lambda_T - 1}{\lambda_1 - 1} = \frac{(1+e_1)^{1/4} - 1}{e_1(1+e_1)^{1/4}} \tag{2.16}$$

Clearly $E^e \to \mu$ for large extensions, but the behavior $E^e \approx 2.5\mu$ for small extensions corresponds to a Young's modulus in an isotropic linear elastic solid with Poisson's ratio 1/4 (Hibbeler, 2000). Indeed, Eq. (2.16) indicates that v^e takes on that value when $e_1 \approx 0$.

3. Indentation problem: plain strain case

Consider that $\Re$ in κ_0 occupies a half-space defined in terms of a fixed Cartesian basis as the region $X_2 > 0$. The smooth motion

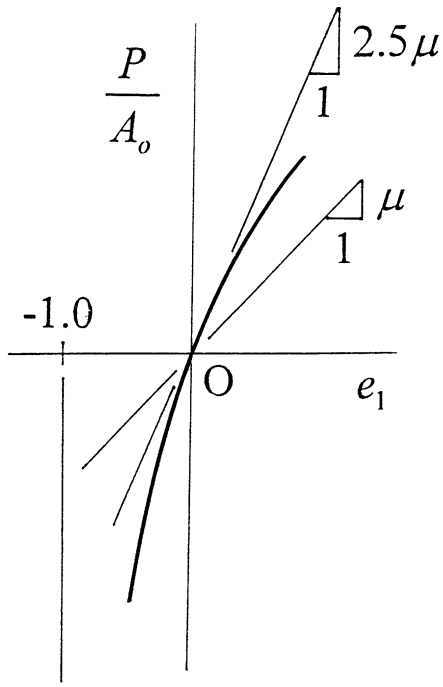

Fig. 1. Compressible neo-Hookean stress–strain curve (uniaxial loading).

$$x_1 = \lambda_1 X_1, \qquad x_2 = \lambda_2 X_2, \qquad x_3 = X_3 \tag{3.1}$$

takes $\mathfrak{R}$ to the plane-strain equilibrium state κ defined by

$$T_{11} = \sigma, \qquad T_{22} = 0, \qquad \lambda_3 = 1 \tag{3.2}$$

where σ is a known constant stress. Clearly $\mathfrak{R}$ now occupies the half-space $x_2 > 0$, and (x_k, λ_k) are the principal coordinates and stretches. For the compressible neo-Hookean model (2.11) and (2.15) considered here, Eqs. (2.1), (2.3), (3.1) and (3.2) combine to produce the results

$$\lambda_2 = \frac{1}{\omega^{1/4}}, \qquad \lambda_1 = \omega\lambda_2, \qquad \omega = \frac{\sigma}{2\mu} + \sqrt{1 + \left(\frac{\sigma}{2\mu}\right)^2} \tag{3.3a}$$

$$T_{33} = \mu\left(\frac{1}{\sqrt{\omega}} - \frac{1}{\omega}\right), \qquad T_{ik} = 0 \quad (i \neq k) \tag{3.3b}$$

required to complete the description of $\mathfrak{R}$ in κ. In Eqs. (3.3a) and (3.3b) it is noted that $0 < \omega \leqslant 1 (\sigma \leqslant 0)$ and $\omega \geqslant 1 (\sigma \geqslant 0)$.

For any superposed infinitesimal deformation $\kappa \to \kappa^*$ of $\mathfrak{R}$, the incremental stresses are given by Eqs. (2.4a) and (2.4b) where, in view on Eqs. (2.5), (2.6), (2.11), (2.15), (3.2), (3.3a) and (3.3b)

$$\lambda'_{1k} = \mu\left(\frac{2}{\omega} - \omega\right), \qquad \lambda'_{2k} = \mu'_{k2} = \frac{\mu}{\omega}, \qquad \lambda'_{3k} = \mu\left(\frac{2}{\omega} - \frac{1}{\sqrt{\omega}}\right), \qquad \mu'_{k1} = \mu\omega, \qquad \mu'_{k3} = \frac{\mu}{\sqrt{\omega}} \tag{3.4}$$

Here $k = (1, 2, 3)$ and all constants in Eq. (3.4) are positive so long as

$$0 < \omega < \sqrt{2} \left(\sigma < \frac{\mu}{\sqrt{2}}\right) \tag{3.5}$$

In the present instance, the infinitesimal deformation occurs when a smooth rigid punch of infinite length and invariant wedge-like profile in the x_3-direction is pressed into the half-space surface $x_2 = 0$ at a constant speed. The wedge apex meets the surface along the line $(x_1, x_2) = 0$ and a contact zone spreads symmetrically with constant sub-critical speed along $x_2 = 0$. A schematic is given in Fig. 2, where $s = v_r(\text{time})$ is the temporal variable, and the constants (C, c) are, respectively, the wedge speed and contact zone expansion rate, each divided by v_r. Here

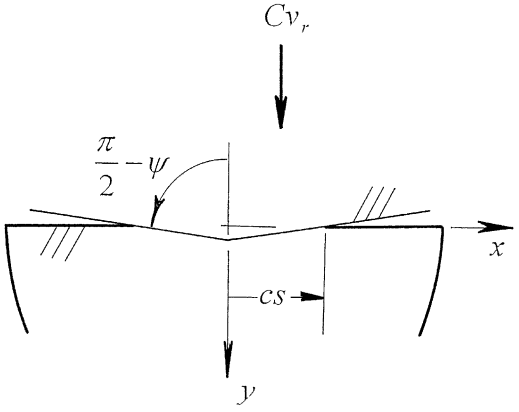

Fig. 2. Schematic of indentation process.

$$v_{\mathrm{r}} = \sqrt{\frac{\mu}{\rho}} \tag{3.6}$$

is the rest value of the rotational wave speed in a linear elastic solid (Achenbach, 1973), so that s has the dimensions of length, and (C, c) are dimensionless. For the moment (3.6) is taken as the critical contact zone expansion rate. Thus, while c is a priori unknown, we require that $0 < c < 1$. Fig. 2 also shows that $s = 0$ defines the instant of initial contact and that, for convenience, the coordinates (x, y, z) are used in place of (x_1, x_2, x_3).

The boundary conditions for the superposed infinitesimal deformations along $y = 0$ can then be written as

$$\mathbf{t}^{(-2)} = 0(|x| > cs); \qquad t_1^{(-2)} = t_3^{(-2)} = 0, \qquad u_2 = Cs - \psi|x| \quad (|x| < cs) \tag{3.7}$$

As depicted in Fig. 2, $\pi/2 - \psi$ is the wedge half-angle, where ψ is assumed to be small enough to justify the approximation $\tan\psi \approx \psi$. The initial conditions for $y > 0$ are

$$\left(u_k, \frac{\partial u_k}{\partial s}\right) \equiv 0 \quad (s \leqslant 0) \tag{3.8}$$

where $k = (1, 2, 3)$. Because the process is plane-strain, only the components (u_1, u_2) of the superposed displacements arise, and these depend only on (x, y, s). Thus, in light of Eqs. (2.4a), (2.4b), (2.8) and (3.4), the relevant governing field equations for $(y, s) > 0$ for the superposed deformation are

$$\frac{1}{\omega}\frac{\partial^2 u_1}{\partial y^2} + \left(\frac{2}{\omega} + \omega\right)\frac{\partial^2 u_1}{\partial x^2} + \frac{2}{\omega}\frac{\partial^2 u_2}{\partial x \partial y} = \frac{\partial^2 u_1}{\partial s^2} \tag{3.9a}$$

$$\frac{2}{\omega}\frac{\partial^2 u_1}{\partial x \partial y} + \frac{3}{\omega}\frac{\partial^2 u_2}{\partial y^2} + \omega\frac{\partial^2 u_2}{\partial x^2} = \frac{\partial^2 u_2}{\partial s^2} \tag{3.9b}$$

where the non-zero elements of $\mathbf{T}'$ are

$$\frac{1}{\mu}T'_{11} = \left(\frac{2}{\omega} + \omega\right)\frac{\partial u_1}{\partial x} + \left(\frac{2}{\omega} - \omega\right)\frac{\partial u_2}{\partial y}, \qquad \frac{1}{\mu}T'_{22} = \frac{1}{\omega}\frac{\partial u_1}{\partial x} + \frac{3}{\omega}\frac{\partial u_2}{\partial y} \tag{3.10a}$$

$$\frac{1}{\mu}T'_{12} = \frac{1}{\mu}T'_{21} = \omega\frac{\partial u_2}{\partial x} + \frac{1}{\omega}\frac{\partial u_1}{\partial y}, \qquad \frac{1}{\mu}T'_{33} = \left(\frac{2}{\omega} - \frac{1}{\sqrt{\omega}}\right)\left(\frac{\partial u_1}{\partial x} + \frac{\partial u_2}{\partial y}\right) \tag{3.10b}$$

Eq. (3.10a) indicates that extensional strain associated with the x-direction depends only on the corresponding traction component when ω achieves the critical value defined by Eq. (3.5). For ω exceeding that value, Eq. (3.10a) implies a negative Poisson effect.

Moreover, Eqs. (3.10a) and (3.10b) show that $\mathrm{tr}\,\mathbf{T}'$ and $\mathrm{tr}\,\mathbf{H}$ are not directly proportional. This indicates the typical (Green and Zerna, 1968; Beatty and Usmani, 1975; Brock, 1999a) result that the superposed deformations are governed by equations analogous to those for a non-isotropic body, although $\mathfrak{R}$ in κ_0 is isotropic.

The mixed boundary conditions along $y = 0$ for this deformation can in view of Eqs. (2.7), (3.2), (3.3a) and (3.3b) be extracted from Eq. (3.7) as

$$T'_{21} - \sigma\frac{\partial u_2}{\partial x} = 0 \tag{3.11a}$$

$$T'_{22} = 0 \quad (|x| > cs) \tag{3.11b}$$

$$u_2 = Cs - \psi|x| \quad (|x| < cs) \tag{3.11c}$$

Eqs. (3.11a)–(3.11c) reflect the fact that $t_3^{(-2)}$ vanishes identically. In addition, we expect the T'_{ik} in Eqs. (3.10a) and (3.10b) to vanish when $\sqrt{x^2+y^2} \to \infty$, $y > 0$ for finite $s > 0$ and to be non-singular and continuous everywhere except the wedge apex $(x, y) = 0$. This latter requirement, as well as the assumption, implicit in Fig. 2 and Eqs. (3.11a)–(3.11c), that multiple contact zones (Brock, 1996) do not in fact arise, can be justified in part by the simple wedge geometry. Finally, the unilateral Signorini conditions (Georgiadis and Barber, 1993) must hold: (a) contact zone normal stress is non-tensile, and (b) indentor and half-space surfaces do not interpenetrate.

4. Plain strain solution candidate

Consider the simpler initial value/boundary value problem governed by Eq. (3.8) to Eqs. (3.10a) and (3.10b), but with Eqs. (3.11a)–(3.11c) replaced by the unmixed conditions

$$T'_{21} - \sigma \frac{\partial u_2}{\partial x} = 0, \qquad T'_{22} = N(x, s) \tag{4.1}$$

along $y = 0$. Clearly, if a function $N(x, s)$ is found such that Eqs. (3.11b) and (3.11c), the boundedness/continuity and Signorini conditions are satisfied, then the simpler problem solution is also that for the infinitesimal deformations in the indentation problem. Conditions Eqs. (3.11b) and (3.11c) require, in particular, that $N(x, s)$ vanish for $|x| > cs$, and satisfaction of Signorini condition (b) implies continuity of $N(x, s)$ as $|x| \to cs-$. In addition, the lack of a characteristic length in the indentation problem and the fact that the only inhomogeneous condition, Eq. (3.11c), is homogeneous of degree 1 in (x, s) suggests that the displacements everywhere are homogeneous of degree 1 in (x, y, s). We choose, therefore, a trial function identical in form to the contact zone stress for the corresponding classical linear elastic indentation problem (Brock, 1978):

$$N(x, s) = \sigma_0 \cosh^{-1} \frac{cs}{|x|} \quad (|x| < cs) \tag{4.2}$$

Here σ_0 is an unknown constant that can be shown by integration of Eq. (4.2) to be the average normal stress on the contact zone.

Solution of the simpler problem in view of Eq. (4.2) should yield a viable candidate for the solution for the superposed infinitesimal deformations. To this end, the unilateral (Sneddon, 1972) and bilateral (van der Pol and Bremmer, 1950) Laplace transforms

$$\hat{F} = \int_0^\infty F \mathrm{e}^{-ps} \mathrm{d}s, \qquad \tilde{F} = \int \hat{F} \mathrm{e}^{-pqx} \mathrm{d}x \tag{4.3}$$

are introduced, along with their corresponding inverse operations

$$F = \frac{1}{2\pi i} \int \hat{F} \mathrm{e}^{ps} \mathrm{d}p, \qquad \hat{F} = \frac{p}{2\pi i} \int \tilde{F} \mathrm{e}^{pqx} \mathrm{d}q \tag{4.4}$$

In Eq. (4.3), the variable p can be taken as real and positive and large enough to ensure existence of the first term in Eq. (4.3), while q is in general complex. In the second term in Eq. (4.3) integration is along the entire x-axis; in Eq. (4.4), it is taken along Bromwich contours in, respectively, the complex p- and q-planes. Application of Eqs. (4.3), (3.9a) and (3.9b) in view of Eqs. (3.8), (3.10a), (3.10b) and (4.1) gives a system of coupled ordinary differential equations whose solution is the double transform set

$$\frac{\mu}{c\sigma_0} p^3 \tilde{u}_k = A_k(q) \mathrm{e}^{-pay} + B_k(q) \mathrm{e}^{-pby} \tag{4.5}$$

for $y > 0$. Here $k = (1, 2)$ and

$$A_1(q) = \frac{qT}{R\sqrt{1-q^2c^2}}, \qquad B_1(q) = -\frac{2qab}{\omega R\sqrt{1-q^2c^2}} \tag{4.6a}$$

$$A_2(q) = -\frac{a}{q}A_1(q), \qquad B_2(q) = \frac{q}{b}B_1(q) \tag{4.6b}$$

where the definitions

$$\sqrt{3}a = \sqrt{\omega}\sqrt{1-q^2c_a^2}, \qquad b = \sqrt{\omega}\sqrt{1-q^2c_b^2} \tag{4.7a}$$

$$T = 1 - q^2\left(\omega + \frac{1}{\omega}\right), \qquad R = \frac{4}{\omega^2}q^2ab + T^2 \tag{4.7b}$$

hold. The dimensionless constants

$$c_b = \sqrt{\omega}, \qquad c_a = \sqrt{\omega + \frac{2}{\omega}} > c_b \tag{4.8}$$

define the effective dilatational and rotational wave speeds $(c_a v_r, c_b v_r)$, respectively, in directions parallel to the x-axis. Boundedness of Eq. (4.5) for $y > 0$ requires that $\mathrm{Re}(a,b) \geqslant 0$ in the q-plane with, respectively, the branch cuts $\mathrm{Im}(q) = 0$, $|\mathrm{Re}(q)| > 1/c_a$ and $\mathrm{Im}(q) = 0$, $|\mathrm{Re}(q)| > 1/c_b$. Here R is a form of the classical (Achenbach, 1973) Rayleigh function. It is analytic in the q-plane with branch cuts $\mathrm{Im}(q) = 0$, $1/c_a < |\mathrm{Re}(q)| < 1/c_b$, and exhibits the roots $q = \pm(1/c_0, 1/c_\mathrm{R})$, where

$$c_0 = \sqrt{\omega - \frac{1}{\omega}}, \qquad c_\mathrm{R} = \sqrt{\omega + \frac{1}{\omega}\left(1 - \frac{2}{\sqrt{3}}\right)} \tag{4.9}$$

For $\sqrt{2/\sqrt{3}-1} < \omega$, $0 < c_\mathrm{R} < c_b$, i.e. $c_\mathrm{R} v_r$ is the effective Rayleigh speed in directions parallel to the x-axis. Thus, sub-critical contact zone expansion is defined by

$$0 < c < c_\mathrm{R} \tag{4.10}$$

For $0 < \omega < \sqrt{2/\sqrt{3}-1}$, however, c_R is imaginary, and so has no meaning as a wave speed. In light of Eq. (4.3), this implies that Rayleigh waves do not exist for pre-stresses

$$\sigma < -2\mu(\sqrt{3}-1)\sqrt{\frac{2}{\sqrt{3}}+1} \tag{4.11}$$

and that indentation in the sense of a sub-critical contact zone expansion rate cannot occur. For $0 < \omega < 1$ $(\sigma < 0)$ c_0 is also imaginary, and so does not correspond to a wave speed. For $1 < \omega < \sqrt{2}$ $(0 < \sigma < \mu/\sqrt{2})$, however, c_0 is real, and $0 < c_0 < c_\mathrm{R}$, but it will be seen that this fact plays no role in solution behavior.

Operation on Eq. (4.5) with the second term of Eq. (4.4) gives the unilateral Laplace transforms $\hat{u}_k$. The analyticity of Eq. (4.5) allows the entire $\mathrm{Im}(q)$-axis to serve as the Bromwich contour, with deformations along semi-circular paths centered at the poles $q = \pm(1/c_0, 1/c_\mathrm{R})$ being introduced when $0 < \omega < 1$ and $0 < \omega < \sqrt{2/\sqrt{3}-1}$, respectively. In any event, the Cagniard–deHoop (deHoop, 1960) scheme allows, in light of exponential decay and Cauchy theory, the integrations to be taken along contours in the q-plane such that the final inversion operation, the first term of Eq. (4.4) can be performed by inspection. The results are that the u_k can be written as the real parts of functions U_k given by

$$\frac{\pi\mu\sqrt{\omega}}{c\sigma_0}U_k = \int_{s_a}^{s} a(q_a)A_k(q_a)\frac{\sqrt{3}(s-t)}{c_a\sqrt{t^2-s_a^2}}\mathrm{d}t + \int_{s_b}^{s} b(q_b)B_k(q_b)\frac{s-t}{c_b\sqrt{t^2-s_b^2}}\mathrm{d}t - i\int_{s_h}^{s_b} b(q_h)B_k(q_h) \times \frac{(s-t)H(s-t)}{c_b\sqrt{s_b^2-t^2}}\mathrm{d}t \quad \left(|x| > \frac{\omega^2 y}{\sqrt{2}}\right) \tag{4.12}$$

for $(y,s) > 0$ and $k = (1,2)$. Here $H(\ )$ is the Heaviside function, and it is understood that an integral vanishes when the lower integration limit exceeds the upper. In Eq. (4.12) t is a positive real variable of integration and

$$r_a^2 q_a = -tx + iy\sqrt{\frac{\omega}{3}}c_a\sqrt{t^2-s_a^2}, \qquad s_a = \frac{r_a}{c_a}, \qquad r_a = \sqrt{x^2 + \frac{\omega}{3}c_a^2 y^2} \tag{4.13a}$$

$$r_b^2 q_b = -tx + iy\sqrt{\omega}c_b\sqrt{t^2-s_b^2}, \qquad s_b = \frac{r_b}{c_b}, \qquad r_b = \sqrt{x^2 + \omega c_b^2 y^2} \tag{4.13b}$$

$$r_b^2 q_h = -tx + y\sqrt{\omega}c_b\sqrt{s_b^2-t^2}, \qquad s_h = \frac{1}{c_a}(|x| + \sqrt{2}y) \tag{4.13c}$$

are parameterization functions for the independent variables. Eqs. (4.13a) and (4.13b) define the upper halves of the branches of hyperbolas in the q-plane. In the isotropic limit ($\omega = 1$), $r_a = r_b = \sqrt{x^2+y^2}$ and the parameterizations reduce to classical (Achenbach, 1973) forms. The parameterization (4.13c) arises to account for the additional contributions caused by the deformation of Eq. (4.13b) around the branch cut of a when $\sqrt{2}|x| > \omega^2 y$.

In light of Eqs. (4.8) and (4.13a), the A_k-terms are dilatational in nature, and occur in the outer expanding semi-elliptical region depicted schematically in Fig. 3a, while Eqs. (4.8) and (4.13b) indicate that the $B_k(q_b)$-terms are rotational, and arise in the inner expanding semi-elliptical region in Fig. 3a. The disturbances associated with the $B_k(q_h)$-terms are the head (bow) wave contributions, and occur in the wedge-shaped regions in Fig. 3a. To confirm the status of Eq. (4.12) as the full field solution for the superposed infinitesimal deformations, Eq. (3.11c) and the Signorini conditions are now imposed.

5. Plane strain solution

Evaluation of (4.12) for $y = 0$, $|x| < cs$ in view of Eqs. (4.13a)–(4.13c) produces simple integrals of real-valued functions. Introduction of the integration variable change $t = 1/v$ then gives

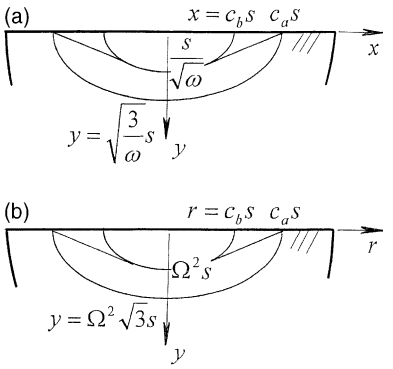

Fig. 3. (a) Wave patterns for plain strain (2D) case. (b) Wave patterns for axially symmetric (3D) case.

$$\mu c_b u_2 = -c\sigma_0 \left[(P)\int_c^{c_a} \frac{\alpha K^2}{vD} \frac{vs - |x|}{\sqrt{v^2 - c^2}} \mathrm{d}v + (P)\int_c^{c_b} \frac{4\alpha^2\beta}{\omega^2 vD} \frac{vs - |x|}{\sqrt{v^2 - c^2}} \mathrm{d}v \right] \tag{5.1}$$

where (P) denoted Cauchy principal value integration, and

$$\sqrt{3}\alpha = \sqrt{\omega}\sqrt{c_a^2 - v^2}, \qquad \beta = \sqrt{\omega}\sqrt{c_b^2 - v^2} \tag{5.2a}$$

$$K = \omega + \frac{1}{\omega} - v^2, \qquad D = \left(K + \frac{2}{\omega}\right)\left(K^2 - \frac{4}{3\omega^2}\right) \tag{5.2b}$$

Because $(|x|, s)$ are independent, substitution of Eq. (5.1) into Eq. (3.11c) gives the two equations necessary to determine the unknowns (c, σ_0). Application of Cauchy residue theory to the v-integrals allows these equations, in fact, to be written in the compact form

$$\left(\frac{\sigma_0}{\mu}, C\right) = \frac{2\psi}{\pi} \frac{1}{\omega^2 - 1} \left[4\omega - \frac{\sqrt{3}(1+\omega^2)^2}{\sqrt{2+\omega^2}}\right] \left(\frac{1}{\omega}, cI\right) \tag{5.3}$$

where I is the real constant

$$I = \int_0^\infty \frac{\mathrm{d}u}{\sqrt{u^2 + c^2}} \frac{(\omega^2 - 1 + \omega u^2)\sqrt{\omega^2 + 2 + \omega u^2}}{4\sqrt{\omega}\sqrt{\omega + u^2}\sqrt{\omega^2 + 2 + \omega u^2} - \sqrt{3}(\omega^2 + 1 + \omega u^2)^2} \tag{5.4}$$

The result (5.4) can be manipulated to give a linear combination of complete elliptic integrals, but little computational or analytical advantage is gained. It should also be noted that the common factor in Eq. (5.3) is indeed finite in the limit as $\omega = 1$. It can be shown for $\sqrt{2/\sqrt{3} - 1} < \omega$ that Eq. (5.3) gives $\sigma_0 < 0$. Thus, Eq. (4.2) satisfies Signorini condition (a). Evaluation of Eq. (4.12) for $y = 0$, $cs < |x| < c_R s$ gives a result similar in form to Eq. (5.1), except that the lower integration limits are now $|x|/s$. Allowing $|x| \to cs+$ in this expression shows that Signorini condition (b) is also satisfied.

6. Indentation problem: axially symmetric case

Consider now that $\mathfrak{R}$ in κ_0 undergoes the smooth motion

$$x_1 = \lambda X_1, \qquad x_2 = \Omega X_2, \qquad x_3 = \lambda X_3 \tag{6.1}$$

into the equilibrium principal stress state κ defined by

$$T_{11} = T_{33} = \sigma, \quad T_{22} = 0 \tag{6.2}$$

where σ is a known constant stress. The generalized neo-Hookean model formulas (2.11) and (2.15) now give in light of Eq. (2.1) and Eqs. (2.4a) and (2.4b) the results

$$\lambda = \frac{1}{\Omega^{3/2}}, \qquad \Omega^4 - \frac{1}{\Omega} + \frac{\sigma}{\mu} = 0, \qquad T_{ik} = 0 \quad (i \neq k) \tag{6.3}$$

required to complete the description of $\mathfrak{R}$ in κ. It is convenient here to use the stretch Ω as a pre-stress parameter instead of the ratio of stretches ω employed in the plane strain formulas (3.3a) and (3.3b). It is also noted that, unlike ω, Ω is the root of a fifth-order polynomial in the second term of Eq. (6.3). Nevertheless, it can be shown that this polynomial exhibits only one positive real root for $\sigma \neq 0$, and that $0 < \Omega \leqslant 1$ $(\sigma \geqslant 0)$ and $\Omega \geqslant 1$ $(\sigma \leqslant 0)$.

For any superposed infinitesimal deformation $\kappa \to \kappa^*$ of $\mathfrak{R}$, the incremental stresses are again given by Eqs. (2.4a) and (2.4b), where now Eqs. (2.5), (2.6), (2.11), (2.15) and (6.3) give

$$\lambda'_{1k} = \lambda'_{3k} = 2\mu\left(\Omega^4 - \frac{1}{2\Omega}\right), \qquad \lambda'_{2k} = \mu'_{k2} = \mu\Omega^4, \qquad \mu'_{k1} = \mu'_{k3} = \frac{\mu}{\Omega} \tag{6.4}$$

Here $k = (1,2,3)$, and all constants are positive so long as

$$\Omega > \frac{1}{2^{1/5}} \quad \left(\sigma < \frac{\mu}{2^{4/5}}\right) \tag{6.5}$$

The infinitesimal deformations now occur when a smooth rigid cone is pressed into the half-space surface $x_2 = 0$ at a constant speed. The cone tip meets the surface at the point $(x_1, x_3) = 0$ and a contact zone spreads in an axially symmetric fashion at a constant sub-critical rate. The schematic in Fig. 2 also suffices to represent this process by showing a typical cross-section, in this case, the $x_3 = 0$ plane. The parameters (s, c, C) retain their previous definitions, therefore, with $0 < c < 1$ being understood for the moment to define sub-critical contact zone expansion. Moreover, the variables (x, y, z) are used in place of (x_1, x_2, x_3). For purposes of generality, the axially symmetric nature of the process is not at this point fully exploited. Therefore, the boundary conditions for the infinitesimal deformations along $y = 0$ are written as

$$\mathbf{t}^{(-2)} = 0 (r > cs); \qquad t_1^{(-2)} = t_3^{(-2)} = 0, \qquad u_2 = Cs - \psi r \quad (r < cs) \tag{6.6}$$

where $r = \sqrt{x^2 + z^2}$ and $\pi/2 - \psi$ is the cone half-angle. Again, the approximation $\tan\psi \approx \psi$ is assumed valid. The initial conditions (3.8) are again valid, but the field equations governing the superposed deformations for $(y, s) > 0$ are now

$$\left[\left(2\Omega^4 + \frac{1}{\Omega}\right)\frac{\partial^2}{\partial x^2} + \Omega^4\frac{\partial^2}{\partial y^2} + \frac{1}{\Omega}\frac{\partial^2}{\partial z^2} - \frac{\partial^2}{\partial s^2}\right]u_1 + 2\Omega^4\frac{\partial}{\partial x}\left(\frac{\partial u_2}{\partial y} + \frac{\partial u_3}{\partial z}\right) = 0 \tag{6.7a}$$

$$\left(\frac{1}{\Omega}\frac{\partial^2}{\partial x^2} + 3\Omega^4\frac{\partial^2}{\partial y^2} + \frac{1}{\Omega}\frac{\partial^2}{\partial z^2} - \frac{\partial^2}{\partial s^2}\right)u_2 + 2\Omega^4\frac{\partial}{\partial y}\left(\frac{\partial u_3}{\partial z} + \frac{\partial u_1}{\partial x}\right) = 0 \tag{6.7b}$$

$$\left[\frac{1}{\Omega}\frac{\partial^2}{\partial x^2} + \Omega^4\frac{\partial^2}{\partial y^2} + \left(2\Omega^4 + \frac{1}{\Omega}\right)\frac{\partial^2}{\partial z^2} - \frac{\partial^2}{\partial s^2}\right]u_3 + 2\Omega^4\frac{\partial}{\partial z}\left(\frac{\partial u_1}{\partial x} + \frac{\partial u_2}{\partial y}\right) = 0 \tag{6.7c}$$

where the constitutive formulas

$$\frac{1}{\mu}T'_{11} = \left(2\Omega^4 + \frac{1}{\Omega}\right)\frac{\partial u_1}{\partial x} + \left(2\Omega^4 - \frac{1}{\Omega}\right)\left(\frac{\partial u_2}{\partial y} + \frac{\partial u_3}{\partial z}\right) \tag{6.8a}$$

$$\frac{1}{\mu}T'_{22} = 3\Omega^4\frac{\partial u_2}{\partial y} + \Omega^4\left(\frac{\partial u_3}{\partial z} + \frac{\partial u_1}{\partial x}\right) \tag{6.8b}$$

$$\frac{1}{\mu}T'_{33} = \left(2\Omega^4 + \frac{1}{\Omega}\right)\frac{\partial u_3}{\partial z} + \left(2\Omega^4 - \frac{1}{\Omega}\right)\left(\frac{\partial u_1}{\partial x} + \frac{\partial u_2}{\partial y}\right) \tag{6.8c}$$

$$\frac{1}{\mu}T'_{12} = \frac{1}{\mu}T'_{21} = \frac{1}{\Omega}\frac{\partial u_2}{\partial x} + \Omega^4\frac{\partial u_1}{\partial y} \tag{6.8d}$$

$$\frac{1}{\mu}T'_{23} = \frac{1}{\mu}T'_{32} = \Omega^4\frac{\partial u_3}{\partial y} + \frac{1}{\Omega}\frac{\partial u_2}{\partial z} \tag{6.8e}$$

$$\frac{1}{\mu}T'_{31}=\frac{1}{\mu}T'_{13}=\frac{1}{\Omega}\left(\frac{\partial u_1}{\partial z}+\frac{\partial u_3}{\partial x}\right) \tag{6.8f}$$

hold. Eqs. (6.8a) and (6.8c) indicate that extensional strains associated with the (x,z)-directions depend only on the corresponding stress components when Ω achieves the critical value defined in Eq. (6.5). For Ω below that value, Eqs. (6.8a) and (6.8c) imply negative Poisson effects. It is seen that $\operatorname{tr}\mathbf{T}'$ and $\operatorname{tr}\mathbf{H}$ are again not proportional, i.e. the isotropy of $\Re$ in κ_0 is lost in the equations for the superposed infinitesimal deformations.

In this case, the more explicit conditions for $y=0$ are

$$T'_{21}-\sigma\frac{\partial u_2}{\partial x}=T'_{23}-\sigma\frac{\partial u_2}{\partial z}=0,\qquad T'_{22}=0\ (r>cs),\qquad u_2=Cs-\psi r\ (r<cs) \tag{6.9}$$

The T'_{ik} are expected to vanish when $\sqrt{x^2+y^2+z^2}\to\infty$, $y>0$ for finite $s>0$, and be non-singular everywhere except the cone tip $(x,y,z)=0$. In addition, the Signorini conditions (a) and (b) must be satisfied.

7. Axially symmetric solution candidate

The simpler problem for the candidate solution now has the unmixed conditions

$$T'_{21}-\sigma\frac{\partial u_2}{\partial x}=T'_{23}-\sigma\frac{\partial u_2}{\partial z}=0,\qquad T'_{22}=N(r,s) \tag{7.1}$$

along $y=0$ in place of Eq. (6.9), where

$$N(r,s)=\sigma_0\cosh^{-1}\frac{cs}{r}\quad(r<cs) \tag{7.2}$$

The form (7.2) is similar to Eq. (4.2), and has the same spatial variation as the contact zone stress for the corresponding static problem (Harding and Sneddon, 1945). Construction of the candidate solution is again accomplished by transform methods, but the bilateral transform, the second term of Eq. (4.3) and its inverse, the second term of Eq. (4.4) are replaced by the multi-variable operations

$$\tilde{F}=\int\int\hat{F}\mathrm{e}^{-p(q_1x+q_3z)}\mathrm{d}x\,\mathrm{d}z, \tag{7.3a}$$

$$\hat{F}=\left(\frac{p}{2\pi i}\right)^2\int\int\tilde{F}\mathrm{e}^{p(q_1x+q_3z)}\mathrm{d}q_1\mathrm{d}q_3 \tag{7.3b}$$

where (q_1,q_3) are in general complex. Application of the first term of Eq. (4.3) and Eq. (7.3a) to Eqs. (6.7a)–(6.7c) in view of Eqs. (7.1), (7.2), (6.8a)–(6.8f) and (3.8) gives the multiple transforms

$$\frac{\mu\Omega^4}{2\pi c^2\sigma_0}p^4\tilde{u}_k=q_kA(q)\mathrm{e}^{-pay}+q_kB(q)\mathrm{e}^{-pby}\quad(k=1,3) \tag{7.4a}$$

$$\frac{\mu\Omega^4}{2\pi c^2\sigma_0}p^4\tilde{u}_2=-aA(q)\mathrm{e}^{-pay}+\frac{q}{b}B(q)\mathrm{e}^{-pby} \tag{7.4b}$$

for $y>0$. Here

$$A(q)=\frac{T}{R(1-q^2c^2)},\quad B(q)=-\frac{2ab}{R(1-q^2c^2)},\quad q^2=q_1^2+q_3^2 \tag{7.5}$$

and the definitions

$$\Omega^2\sqrt{3}a = \sqrt{1-q^2c_a^2}, \qquad \Omega^2 b = \sqrt{1-q^2c_b^2} \tag{7.6a}$$

$$\Omega^4 T = 1 - q^2\left(\Omega^4 + \frac{1}{\Omega}\right), \qquad R = 4q^2ab + T^2 \tag{7.6b}$$

hold. The dimensionless constants

$$c_b = \frac{1}{\sqrt{\Omega}}, \qquad c_a = \sqrt{\frac{1}{\Omega} + 2\Omega^4} > c_b \tag{7.7}$$

define the effective rotational and dilatational wave speeds $(c_b v_r, c_a v_r)$, respectively, parallel to the plane $y = 0$. Boundedness of Eqs. (7.4a) and (7.4b) for $y > 0$ requires that $\mathrm{Re}(a,b) \geqslant 0$ in the q-plane with branch cuts $\mathrm{Im}(q) = 0$, $|\mathrm{Re}(q)| > 1/c_a$ and $\mathrm{Im}(q) = 0$, $|\mathrm{Re}(q)| > 1/c_b$, respectively. The term R is again a form of the classical Rayleigh function; it is analytic in the q-plane with branch cuts $\mathrm{Im}(q) = 0$, $1/c_a < |\mathrm{Re}(q)| < 1/c_b$, with roots $q = \pm(1/c_0, 1/c_\mathrm{R})$, where

$$c_0 = \sqrt{\frac{1}{\Omega} - \Omega^4}, \qquad c_\mathrm{R} = \sqrt{\frac{1}{\Omega} + \Omega^4\left(1 - \frac{2}{\sqrt{3}}\right)} \tag{7.8}$$

For $0 < \Omega < (2/\sqrt{3} - 1)^{-1/5}$ it can be shown that $0 < c_\mathrm{R} < c_b$, i.e. $c_\mathrm{R} v_r$ is the effective Rayleigh wave speed parallel to the plane $y = 0$. Thus, sub-critical expansion is again defined by Eq. (4.10), where Eq. (7.8) now holds. For $\Omega > (2/\sqrt{3} - 1)^{-1/5}$, however, c_R is imaginary and has no meaning as a wave speed. In light of Eq. (6.3) this implies that Rayleigh waves do not exist for pre-stresses

$$\sigma < 2\mu\left(\frac{1}{\sqrt{3}} - 1\right)\left(\frac{2}{\sqrt{3}} - 1\right)^{-4/5} \tag{7.9}$$

and that, as in the plane strain case, sub-critical contact zone expansion cannot occur. For $\Omega > 1$ $(\sigma < 0)$ c_0 is also imaginary, and so does not correspond to a wave speed. For $2^{-1/5} < \Omega < 1$ $(0 < \sigma < 2^{-4/5}\mu)$, however, c_0 is real and $0 < c_0 < c_\mathrm{R}$, but plays no role in solution behavior.

Operation on Eqs. (7.4a) and (7.4b) with Eq. (7.3b) and use of the Cagniard–deHoop technique (de-Hoop, 1960) gives, in a manner similar to that for the plane strain case, u_k that are the real parts of functions U_k, where

$$\begin{aligned}\frac{\pi\mu\Omega^2}{2c^2\sigma_0}\left(\frac{r}{x}U_1, \frac{r}{z}U_3\right) = &-\int_0^{u_a}\mathrm{d}u\int_{s_a}^{s} Q_a a(q_a)A(q_a)\frac{\sqrt{3}(s-t)}{c_a\sqrt{t^2-s_a^2}}\mathrm{d}t - \int_0^{u_b}\mathrm{d}u\int_{s_b}^{s} Q_b b(q_b)B(q_b)\frac{s-t}{c_b\sqrt{t^2-s_b^2}}\mathrm{d}t \\ &+ i\int_0^{u_h}\mathrm{d}u\int_{s_h}^{s_b} Q_h b(q_h)B(q_h)\frac{(s-t)H(s-t)}{c_b\sqrt{s_b^2-t^2}}\left(r > \frac{y}{\Omega^5\sqrt{2}}\right)\end{aligned} \tag{7.10a}$$

$$\begin{aligned}\frac{\pi\mu\Omega^2}{2c^2\sigma_0}U_2 = &\int_0^{u_a}\mathrm{d}u\int_{s_a}^{s} a^2(q_a)A(q_a)\frac{\sqrt{3}(s-t)}{c_a\sqrt{t^2-s_a^2}}\mathrm{d}t - \int_0^{u_b}\mathrm{d}u\int_{s_b}^{s} q_b B(q_b)\frac{s-t}{c_b\sqrt{t^2-s_b^2}}\mathrm{d}t \\ &+ i\int_0^{u_h}\mathrm{d}u\int_{s_h}^{s_b} q_h B(q_h)\frac{(s-t)H(s-t)}{c_b\sqrt{s_b^2-t^2}}\mathrm{d}t\left(r > \frac{y}{\Omega^5\sqrt{2}}\right)\end{aligned} \tag{7.10b}$$

for $(y,s) > 0$. In Eqs. (7.10a) and (7.10b) (u,t) are real variables, it is understood that integrals vanish when the lower integration limits exceed the upper, and

$$q_a^2 = Q_a^2 - u^2, \quad q_b^2 = Q_b^2 - u^2, \quad q_h^2 = Q_h^2 - u^2 \tag{7.11}$$

Here the parameterization functions are

$$R_a^2 Q_a = -tr + \mathrm{i}\frac{c_a y}{\Omega^2\sqrt{3}}\sqrt{t^2 - s_a^2}, \qquad s_a = R_a\sqrt{u^2 + \frac{1}{c_a^2}}, \qquad R_a = \sqrt{r^2 + \frac{c_a^2 y^2}{3\Omega^4}} \tag{7.12a}$$

$$R_b^2 Q_b = -tr + \mathrm{i}\frac{c_b y}{\Omega^2}\sqrt{t^2 - s_b^2}, \qquad s_b = R_b\sqrt{u^2 + \frac{1}{c_b^2}}, \qquad R_b = \sqrt{r^2 + \frac{c_b^2 y^2}{\Omega^4}} \tag{7.12b}$$

$$R_b^2 Q_h = -tr + \frac{c_b y}{\Omega^2}\sqrt{s_b^2 - t^2}, \qquad s_h = r\sqrt{u^2 + \frac{1}{c_a^2}} + \frac{\sqrt{2\Omega}}{c_a} y \tag{7.12c}$$

where the integration limits

$$u_a = \sqrt{\left(\frac{s}{R_a}\right)^2 - \frac{1}{c_a^2}}, \quad u_b = \sqrt{\left(\frac{s}{R_b}\right)^2 - \frac{1}{c_b^2}}, \quad u_h = \frac{1}{c_a y}\sqrt{2\Omega^{10} r^2 - y^2} \tag{7.13}$$

vanish when the arguments in the radicals vanish or become negative. The schematic in Fig. 3b shows the wave fronts associated with Eqs. (7.10a) and (7.10b). The A- and $B(q_b)$-terms are, respectively, dilatational and rotational in nature and arise within the outer and inner, respectively, expanding ellipsoidal regions. The $B(q_h)$-terms represent head wave disturbances that arise within the expanding wedge-like toroidal regions.

8. Axially symmetric solution

Evaluation of Eq. (7.10b) for $y = 0$, $r < cs$ in light of Eqs. (7.11)–(7.13) is simpler than its form suggests because the parameterization functions (Q_a, Q_b, Q_h) become both real and independent of u. Indeed, the resulting u-integrations can now be performed explicitly, whereupon introduction of the integration variable change $t = 1/v$ gives

$$\begin{aligned}\frac{\pi\mu\Omega^4}{2c^2\sigma_0} u_2 = &-(P)\int_{r/s}^{c_a} \frac{\alpha K^2}{vD}\frac{\mathrm{d}v}{v^2 - c^2}\left[vs\ln\left(\frac{vs}{r} + \sqrt{\frac{v^2 s^2}{r^2} - 1}\right) - \sqrt{v^2 s^2 - r^2}\right] \\ &-(P)\int_{r/s}^{c_b} \frac{4\alpha^2\beta}{vD}\frac{\mathrm{d}v}{v^2 - c^2}\left[vs\ln\left(\frac{vs}{r} + \sqrt{\frac{v^2 s^2}{r^2} - 1}\right) - \sqrt{v^2 s^2 - r^2}\right]\end{aligned} \tag{8.1}$$

for $y = 0$, $r < cs$, where

$$\Omega^2\sqrt{3}\alpha = \sqrt{c_a^2 - v^2}, \quad \Omega^2\beta = \sqrt{c_b^2 - v^2} \tag{8.2a}$$

$$\Omega^4 K = \Omega^4 + \frac{1}{\Omega} - v^2, \quad D = (K+2)\left(K^2 - \frac{4}{3}\right) \tag{8.2b}$$

In contrast to its plane-strain counterpart (5.1), Eq. (8.1) does not appear to be linear in (r, s), although it is appropriately homogeneous of degree 1. Similar forms arise in the analysis of axially symmetric crack growth (Brock, 1991), however, and use of Cauchy residue theory shows that Eq. (8.1) is indeed linear when $r < cs$. Substitution into the third term of Eq. (6.9) then gives the two formulas

$$\left(\frac{\sigma_0}{\mu}, C\right) = \frac{\psi}{1 - \Omega^5}\left[4\Omega^5 - \frac{\sqrt{3}(1 + \Omega^5)^2}{\sqrt{1 + 2\Omega^5}}\right]\left(\Omega^{3/2}, \frac{c^2}{2} I\right) \tag{8.3}$$

necessary to find (σ_0, c), where I is the real constant

$$I = \int_0^\infty \frac{\mathrm{d}u}{u^2 + c^2} \frac{(1 - \Omega^5 + \Omega u^2)\sqrt{1 + 2\Omega^5 + \Omega u^2}}{4\Omega^5\sqrt{1 + \Omega u^2}\sqrt{1 + 2\Omega^5 + \Omega u^2} - \sqrt{3}(1 + \Omega^5 + \Omega u^2)^2} \tag{8.4}$$

The integration (8.4) can actually be performed analytically, but the resulting combination of logarithmic and arctangent functions of (c, Ω) offer limited computational and analytical advantage. It can be shown that the common factor in (8.3) is finite in the limit as $\Omega = 1$, and that $\sigma_0 < 0$ when $0 < \Omega < (2/\sqrt{3} - 1)^{-1/5}$. Thus, Eq. (7.2) satisfies Signorini condition (a). For $y = 0$, $cs < r < c_R s$ it can be shown that Eq. (8.1) satisfies Signorini condition (b).

9. Comments and comparisons

To this point, the exact transient full-field solutions for two cases of indentation of pre-stressed hyperelastic half-spaces have been presented. The material chosen for illustration is an isotropic compressible neo-Hookean solid, and both cases have been treated as the superposition of indentation-triggered infinitesimal deformations upon the (possibly) finite deformation due to pre-stress. The equations governing the superposed deformations, Eqs. (3.9a) and (3.9b) and Eqs. (3.10a) and (3.10b) for plane strain and Eqs. (6.7a)–(6.7c) and Eqs. (6.8a)–(6.8f) for axial symmetry, are non-isotropic in nature, and give rise to elliptical or ellipsoidal dilatational and rotational wave patterns, and head waves in classical (Achenbach, 1973) wedge-like regions. Moreover, the compressive contact zone stresses for the two cases are similar in form, and lead to constant average values.

Despite these similarities, the two indentation processes are not the same and, indeed, the effective elastic constants arising in Eqs. (3.9a) and (3.9b) and Eqs. (3.10a) and (3.10b) differ from those in Eqs. (6.7a)–(6.7c) and Eqs. (6.8a)–(6.8f). As a manifestation of this, consider the dimensionless constants (c_b, c_a, c_R) given by Eqs. (4.8) and (4.9) in light of Eqs. (3.3a) and (3.3b) for plane strain, and by Eqs. (7.7) and (7.8) in light of Eq. (6.3) for the axially symmetric case. These are associated with, respectively, the rotational, dilatational and Rayleigh wave speeds in the deformed configuration, and are plotted vs. pre-stress in Fig. 4. There the plane strain case is denoted by 2D (broken line) and the axially symmetric cases, by 3D (solid line). The allowable ranges of pre-stress are defined by Eqs. (3.5) and (4.11) for the 2D case, and Eqs. (6.5) and (7.9) for the 3D case, i.e. the ranges for which the Poisson effect is not negative and Rayleigh waves exist.

Fig. 4 shows that the Rayleigh waves exist for a substantially larger range of compressive pre-stress in the 3D case, but that the onset of the negative Poisson effect occurs for a slightly larger tensile pre-stress in the 2D case. The behavior of (c_b, c_a, c_R) shows that, for both cases, compressive pre-stress increases the dilatational wave speed, and a tensile pre-stress decreases it, while the situation is reversed for the rotational and Rayleigh wave speeds. In the limit as the pre-stress vanishes, speeds for the two cases are identical, but the changes in all three speeds due to pre-stress are greater for the 2D case. That is, the constraint imposed by plane strain enhances the effects of pre-stress.

Differences in behavior are also seen for the average contact zone stresses given by Eqs. (5.3) and (8.3). In Fig. 5 these constants are plotted for the two cases over the allowable ranges of pre-stress. Again, the values are identical in the absence of pre-stress, and both vanish when the pre-stress reaches the critical compressive value at which Rayleigh waves disappear. The behavior for the two cases is otherwise distinct. For the 3D case, the average contact stress drops for both tensile and compressive pre-stresses, while it actually increases in the 2D case for tensile pre-stress. That is, for a given indentation speed and apex angle, the constraint imposed by plane strain requires a greater average contact stress under a tensile pre-stress.

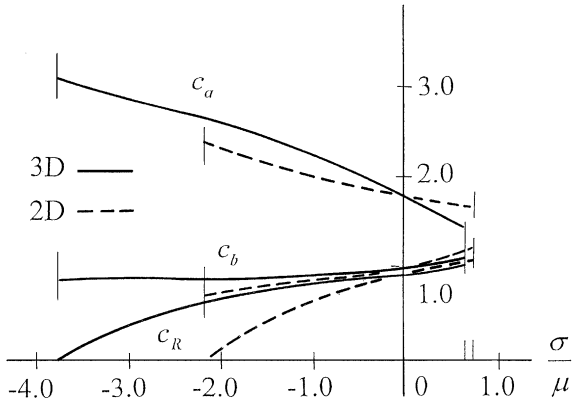

Fig. 4. Variation of effective wave speeds with pre-stress.

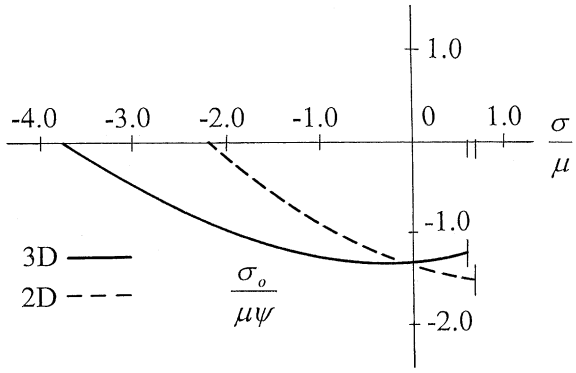

Fig. 5. Variation of average contact zone stress with pre-stress.

Figs. 4 and 5 show clearly that the effects of pre-stress are small for pre-stress magnitudes small in comparison with the shear modulus μ. Indeed, the critical pre-stress values for Rayleigh wave annihilation and negative Poisson effects are of $O(\mu)$. Nevertheless, the trends indicated are important, especially in the context of hyper-elasticity.

In regard to the analysis itself, it is convenient that the neo-Hookean model used to represent the hyper-elastic solid gives governing equations for the superposed infinitesimal deformations whose non-isotropic nature did not preclude simple exact expressions for the dilatational, rotational and Rayleigh wave speeds. Similarly, the parameterization functions occurring in the full-field solutions are similar in form to the classical (deHoop, 1960) results for linear isotropic elasticity.

In this analysis, the plane strain solutions were formulated in terms of a ratio of stretches induced by pre-stress, while one of the stretches itself was used for the axially symmetric case. Both quantities can, of course, be related to the pre-stress; in the plane strain case, explicitly; in the axially symmetric case, as the root of a fifth-order polynomial. The approach used here allowed both cases to be described with simple functions of integral powers of the given pre-stress parameter.

In summary, then, both the existence of pre-stress and its type are important in the transient indentation of hyper-elastic surfaces; in particular, the constraint imposed by plane strain enhances the role of pre-stress in solution response.

References

Achenbach, J.D., 1973. Wave Propagation in Elastic Solids. North-Holland/American Elsevier, Amsterdam.
Barber, J.R., 1996. Surface displacements due to a steadily moving point force. ASME Journal of Applied Mechanics 63, 245–251.
Beatty, M.F., Usmani, S.A., 1975. On the indentation of a highly elastic half-space. Quarterly Journal of Mechanics and Applied Mathematics 28, 47–62.
Brock, L.M., 1978. Frictionless indentation by an elastic punch: a dynamic Hertzian contact problem. Journal of Elasticity 8, 381–392.
Brock, L.M., 1991. Exact transient results for penny-shaped crack growth under combined loading. International Journal of Solids and Structures 28, 517–531.
Brock, L.M., 1996. Some analytical results for heating due to irregular sliding contact of thermoelastic solids. Indian Journal of Pure and Applied Mathematics 27, 1257–1278.
Brock, L.M., 1999a. Rapid sliding indentation with friction of a pre-stressed thermoelastic material. Journal of Elasticity 53, 161–188.
Brock, L.M., 1999b. Sliding contact with friction at arbitrary constant speeds on a pre-stressed highly elastic half-space. Journal of Elasticity 57, 105–132.
Brock, L.M., 2001. Rapid sliding contact on a highly elastic pre-stressed material. International Journal of Non-Linear Mechanics, in press.
deHoop, A.T., 1960. A modification of Cagniard's method for seismic pulse problems. Appl. Sci. Res. B8, 349–356.
Georgiadis, H.G., Barber, J.R., 1993. On the super-Rayleigh/subseismic elastodynamic indentation problem. J. Elast. 31, 141–161.
Green, A.E., Zerna, W., 1968. Theoretical Elasticity, second ed., Oxford University Press, London.
Harding, J.W., Sneddon, I.N., 1945. The elastic stresses produced by the indentation of the plane surface of a semi-infinite elastic solid by a rigid punch. Proceedings of the Cambridge Philosophical Society 41, 16–26.
Hibbeler, R.C., 2000. Mechanics of Materials, fourth ed., Prentice Hall, NJ.
Sneddon, I.N., 1972. The Use of Integral Transforms. McGraw-Hill, New York.
Truesdell, C., Noll, W., 1965. The non-linear field theories of mechanics, in: Flugge, W. (Ed.), Handbuch der Physik III/3, Springer, Berlin.
Pol, B., Bremmer, H., 1950. Operations Based on the Two-Side Laplace Integral. Cambridge University Press, Cambridge.
Willis, J.R., 1973. Self-similar problems in elastodynamics. Philosophical Transactions of the Royal Society of London A274, 435–491.